

A study of the angular resolution of GRAPES-3 EAS array

V.B. Jhansi,^{a,h,*} S. Ahmad,^{a,c} M. Chakraborty,^{a,b} S.R. Dugad,^{a,b} S.K. Gupta,^{a,b} B. Hariharan,^{a,b} Y. Hayashi,^{a,d} P. Jagadeesan,^{a,b} A. Jain,^{a,b} P. Jain,^{a,e} S. Kawakami,^{a,d} H. Kojima,^{a,f} S. Mahapatra,^{a,g} P.K. Mohanty,^{a,b,1} S.D. Morris,^{a,b} P.K. Nayak,^{a,b} A. Oshima,^{a,f} D. Pattanaik,^{a,b,g} P.S. Rakshe,^{a,b} K. Ramesh,^{a,b} B.S. Rao,^{a,b} L.V. Reddy,^{a,b} S. Shibata,^{a,f} F. Varsi^{a,e} and M. Zuberi^{a,b}

^aThe GRAPES-3 Experiment, Cosmic Ray Laboratory, Raj Bhavan, Ooty 643001, India

^bTata Institute of Fundamental Research, Dr. Homi Bhabha Road, Mumbai 400005, India

^cAligarh Muslim University, Aligarh 202002, India

^dGraduate School of Science, Osaka City University, Osaka 558-8585, Japan

^eIndian Institute of Technology Kanpur, Kanpur 208016, India

^fCollege of Engineering, Chubu University, Kasugai, Aichi 487-8501, Japan

^gUtkal University, Bhubaneswar 751004, India

^hKhalifa University, P.O. Box 127788, Abu Dhabi, United Arab Emirates

E-mail: jhansi.bhavani@ku.ac.ae

The sensitivity with which the γ ray sources can be studied is inversely proportional to the angular resolution of an extensive air shower (EAS) array. Therefore it is important to determine the EAS arrival direction as accurately as possible. In this paper, we present the methods that were recently implemented by GRAPES-3 experiment to improve its angular resolution. In the GRAPES-3 experiment, consisting of an array of ~ 400 scintillator detectors, the arrival direction of the shower is determined from the relative arrival times of particles at different detectors. The arrival times measured by each detector is initially corrected for the fixed arrival time caused by the cables connecting the individual detectors to their respective time-to-digital converter channels. A new method was developed based on the random walk technique to measure these fixed arrival times with a smaller uncertainty. A study based on simulations was also performed to verify the efficacy of this method. The arrival times were further corrected for the conical shape of the shower front, the slope of which had exhibited a strong dependence on the shower size and age. The correction for these dependencies led to an improvement in the angular resolution of the array by a factor of ~ 2 . The angular resolution of GRAPES-3 array obtained through array division methods is 0.8° for energies $E > 5$ TeV, which improves to 0.3° at $E > 100$ TeV, and finally approaches 0.2° at $E > 500$ TeV.

38th International Cosmic Ray Conference (ICRC2023)
26 July - 3 August, 2023
Nagoya, Japan



*Speaker

1. Introduction

In the extensive air shower technique, the γ ray flux has to be detected against a huge background of isotropic cosmic rays. To view a point source with good sensitivity, the signal to noise ratio has to be maximized, either by increasing the area of detection, or by improving the angular resolution [1]. The signal to noise ratio is inversely proportional to the angular resolution. Therefore, it is of utmost importance to determine the arrival direction as accurately as possible. The GRAPES-3 (Gamma Ray Astronomy at PeV EnergyS Phase-3) experiment is primarily designed to study the cosmic ray sources in the \sim TeV-PeV energy range. The experiment is located at Ooty (11.4⁰N latitude, 76.7⁰E longitude) at an altitude of 2200 m above the mean sea level. The experiment consists of a densely packed EAS array, and a large area muon telescope. In this array, \sim 400 scintillator detectors are arranged in the form of concentric hexagonal rings, with a separation of 8 m between the adjacent detectors. Details of the detector set-up, trigger and electronics are discussed elsewhere [2]. An active area of 2% makes GRAPES-3 one of the densest arrays of the world. In comparison, experiments such as KASCADE, CASA MIA, GAMMA, EAS-TOP etc have an active area of only \sim 1%. A large active area is beneficial for achieving an improved angular resolution [1].

When an EAS lands on an array, each detector measures the number of EAS particles passing through it, and their arrival times with respect to the trigger signal. The arrival direction of a shower is determined from the relative arrival times of particles in the shower front. Therefore precise arrival time measurements are required for obtaining an improved angular resolution.

2. Measurement of TDC Offset from EAS data

The time measured in each detector is the sum of arrival times of particles and the time taken for the signal to be transferred from the detector to the HPTDC [4][3]. The quantity mentioned later, referred to as TDCZero varies significantly from detector to detector due to unequal propagation delays in the signal cable, as well as due to dissimilar electronics delays. The distribution of the difference in arrival times (Δt) of any two detectors represents the projected angular distribution of air showers projected on to the vertical plane containing the two detectors, and the centroid of this distribution gives the relative TDCZero [1]. Hence, it is possible to determine the relative TDCZero for any two neighbouring detectors in the array by estimating the peak of the Δt distribution, in which case the effective Δt (in ns) is calculated as $\Delta t = \Delta t + \Delta z \times 3.33$ where z corresponds to the z coordinates of the detectors (in meters). The Δt distribution for detector pair 9-20 is shown in Fig. 1(a). The Δt distribution is then fitted with a Gaussian function to obtain its peak value $(\Delta t)_p$.

To calculate the TDCZero for every detector relative to a common detector, we have developed a new technique called the random walk method which can be described as follows. Nearly, every detector in the array has twelve neighbours at a distance of 16 m. Starting from a reference detector, its time offset relative to any of the twelve neighbours is calculated by generating an integer random number in the range of 1-12. Depending on the value generated, corresponding neighbour is selected, and their relative time offset is measured. Next, another random number is generated to select the neighbour of the previously selected detector. This procedure is repeated until the reference detector is reached. This procedure is terminated if the array boundary is reached or if the reference detector is not reached in 100 steps. For each step, we keep on adding the $(\Delta t)_p$ values

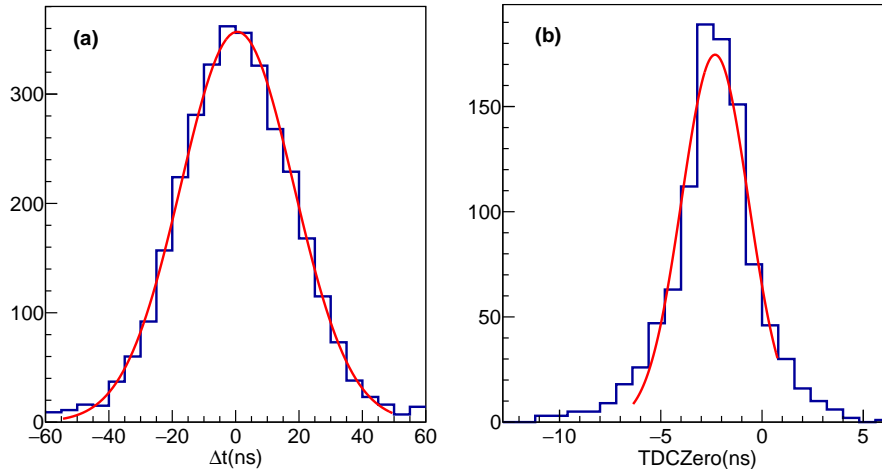


Figure 1: (a) Distribution of particle arrival time differences for detectors 9 and 20 for 1 hour. Gaussian fit to data yields a peak at (0.5 ± 0.3) ns and σ of 17.8 ns, (b) Distribution of TDCZero for detector 25 relative to reference detector 9 based on 1000 random walks. The peak from a Gaussian fit occurs at (-2.31 ± 0.06) ns.

measured directly from the EAS data to finally obtain the net $(\Delta t)_p$ between reference and starting detector. Next, the process is repeated, and the net $(\Delta t)_p$ is calculated but it follows a different path because of the use of random numbers. Thus, by repeating this procedure, net $(\Delta t)_p$ is calculated for 1000 paths and its mean gives a precise value of the time offset namely, the TDCZero. By repeating this procedure the TDCZero of every detector is calculated relative to the reference detector.

The above technique can be illustrated by an example. If detector 9 is taken to be the reference detector. We seek to determine the TDCZero of all detectors relative to the reference detector. For example, let us determine the TDCZero of detector 25 relative to reference detector 9. Detector 25 can be reached from 9 by a path passing through the nearest neighbours in certain number of steps, where each neighbor is selected using random numbers. This may be written mathematically for one random path as follows,

$$(\Delta t)_p^{9-25} = (\Delta t)_p^{9-7} + (\Delta t)_p^{7-33} + (\Delta t)_p^{33-15} + \dots \dots \dots (\Delta t)_p^{43-70} + (\Delta t)_p^{70-25} \quad (1)$$

The TDCZero is obtained by using a large number of random paths generated through nearest neighbours and by calculating the mean $(\Delta t)_p$ as shown in Fig. 1(b).

To verify the effectiveness of the random walk method, about 10 million proton showers were simulated in the energy range of 10-1000 TeV using CORSIKA package, with zenith angle $\theta < 60^\circ$ and a spectral index $\gamma=2.7$. The EAS cores were then distributed randomly over a large circular area of radius 120 m. This procedure was repeated 10 times with different random seeds. Hence, in total, 100 million showers, were used for the analysis. It is to be noted that the CORSIKA package provides with the arrival times of EAS particles on an horizontal surface, at a given atmospheric depth. However, the Z coordinates of the detectors differ from one another, and the arrival times of the EAS particles at various detectors were modified accordingly. The details of this correction method is reported elsewhere [7]. The arrival time of the particle that passes first through the detector, is approximated as the arrival time of the shower front for that detector location. In addition, the number of particles passing through each detector is converted into an equivalent

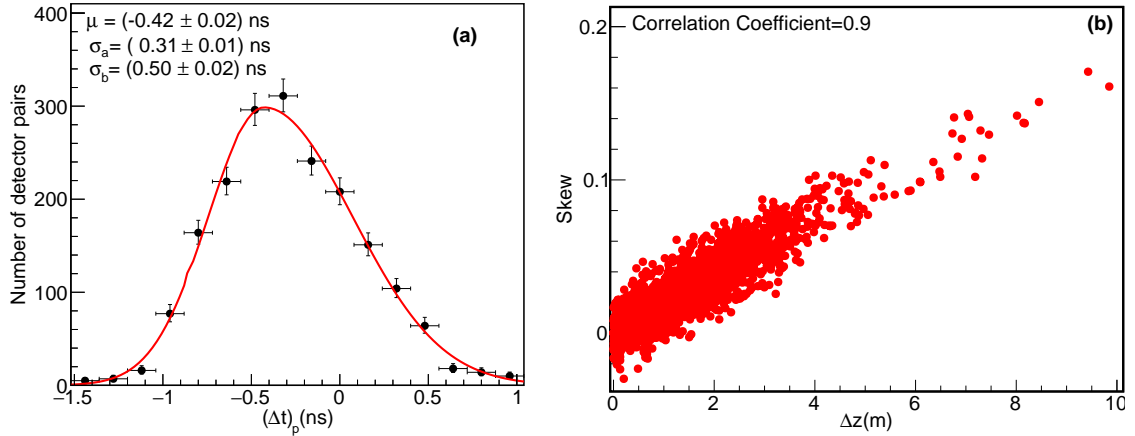


Figure 2: (a) The distribution of $(\Delta t)_p$ of neighbouring detector pairs from simulations. A bifurcated Gaussian fit to this distribution yields a peak at (-0.42 ± 0.02) ns. (b) Variation of skew of Δt distribution of neighbouring detector pairs as a function of difference in their Z coordinates (Δz). The skew increases with Δz with a high correlation coefficient of 0.9.

signal based on the integrated charge distribution from single muons. It is to be noted that the Level-0 and Level-1 trigger logic were also implemented to generate the EAS trigger, and was used as a definitive criteria for the shower selection processes.

In the case of simulations it is expected that the peak of Δt distribution of neighbouring pairs should occur at zero. The distribution of the peak $(\Delta t)_p$ values obtained by fitting the Δt distribution with a Gaussian function is shown in Fig. 2(a). This distribution when fitted by a bifurcated Gaussian function (a Gaussian with different widths to the left and right of its mean) yields a mean value of (-0.42 ± 0.02) ns and widths of $\sigma_a = (0.31 \pm 0.01)$ ns and $\sigma_b = (0.50 \pm 0.02)$ ns on the left and right side of the mean respectively. In addition, it is observed that the skew of Δt distribution has a strong dependence on the difference in their Z coordinates (Δz) as shown in Fig. 2(b) with a correlation coefficient of 0.9. The same effect is observed for the neighbouring detectors in the EAS data. However, the correction for the arrival direction of the shower has led to significant reduction in the width of the $(\Delta t)_p$ distribution as shown in Fig. 3(a). Also the mean of this distribution obtained from a fit to a Crystal Ball function [5] is (-0.030 ± 0.008) ns, which is very close to the expected null value. Moreover, the skew also does not increase with Δz . As a result, the correlation coefficient of the skew and Δz reduces to a negligible value of 0.1 as shown in Fig. 3(b). In the case of data, the arrival direction of the shower is not known before reconstruction and hence, initially we find its direction by using less accurate values of TDCZeros calculated earlier. After obtaining the approximate direction of the shower, corrections are implemented for inclined showers. Consequently, the skew becomes negligible and more accurate values of TDCZeros are obtained.

3. Determination of shower front curvature

The slope of the shower front is obtained from a linear fit to the time residuals with respect to planar fit. To investigate the dependence of shower slope on shower size N_e and age, a total

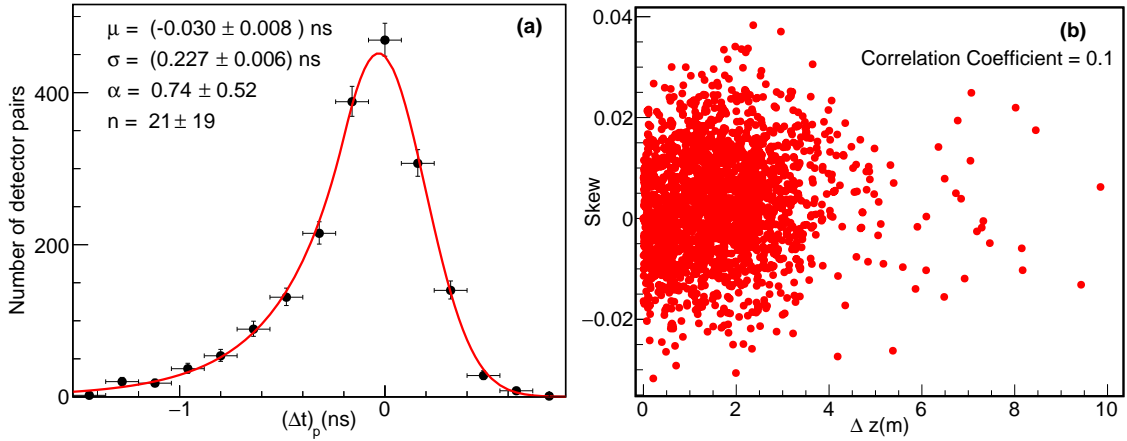


Figure 3: (a) Distribution of $(\Delta t)_p$ from simulations after correcting for the EAS arrival direction. The distribution is fitted with a Crystal Ball function [5] which yields a peak value of $(-0.030 \pm 0.008) \text{ ns}$ and a σ of $(0.227 \pm 0.006) \text{ ns}$. (b) The skew of Δt distributon of neighbouring detector pairs shows no dependence on the difference in Z coordinates (Δz) as expected. The skew is independent of Δz as attested by a low correlation coefficient of 0.1.

Table 1: The functional dependence of M_{N_e} and C_{N_e} on shower size N_e

Variable	Functional Form	Fitted Parameters
M_{N_e}	$a_1 \exp(-b_1 n_e) + c_1 \exp(-d_1 n_e^2) - 1$	$a_1=0.791, b_1=-0.003, c_1=0.789, d_1=0.216$
C_{N_e}	$1 - a_2 \exp(-b_2 n_e) - c_2 \exp(-d_2 n_e^2)$	$a_2=0.479, b_2=-0.010, c_2=1.290, d_2=0.176$

$\dagger n_e = \log_{10}(N_e)$

\dagger The units of a_1, c_1, a_2, c_2 are ns/m

of about 10^9 EAS, collected during 2014 from January 1 to December 31 were categorized into 20 shower size bins each with a width of 0.1 on logarithmic scale. The variation of shower front curvature slope with respect to the age and size are shown in Fig. 4. Following major inferences can be drawn from Fig. 4, (1) the slope falls with age in each size bin, (2) the slope is larger for larger shower size for a given age. The variation of slope with age in each size bin is first parametrized by the equation $\alpha_{\text{age}}^{N_e} = M_{N_e} \cdot \text{age} + C_{N_e}$. The parameters M_{N_e} and C_{N_e} are calculated for each size bin. The observed variation of M_{N_e} and C_{N_e} with size has also been parametrized by similar functional form as mentioned in Table 1. It is to be noted that the outliers have been eliminated based on the dependence of the slope on size and age. The percentage of outliers gradually increases with shower size (9.7–13.3)%. A study was also carried out to obtain the variation of M_{N_e} and C_{N_e} with the zenith angle (θ). For this purpose the data were divided into five $\sec(\theta)$ bins of width 0.1 from 1 to 1.5.

4. Angular resolution of GRAPES-3

The angular resolution of the GRAPES-3 array was obtained by employing two different methods, namely, (1) odd-even (oe), (2) left-right (lr). The results obtained by these two methods were corroborated by detailed Monte Carlo simulations of EAS using CORSIKA. In the odd-even

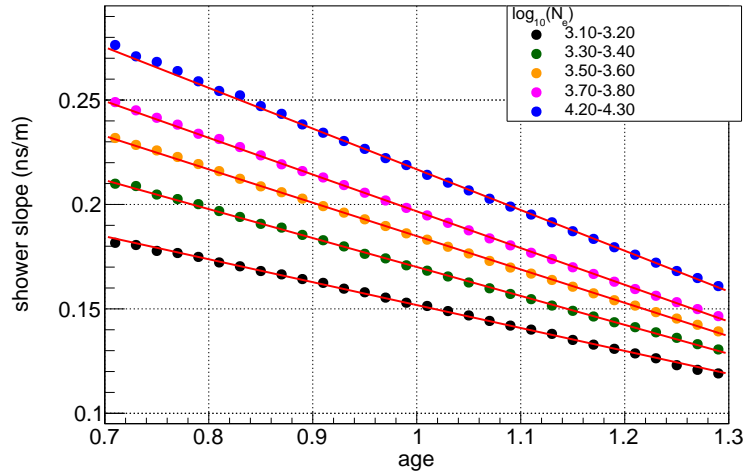


Figure 4: Dependence of shower slope on EAS age for five size (N_e) groups. A linear fit is performed for each size group to obtain the slope M_{N_e} and intercept C_{N_e} (partly adapted from [6])

method, the array is first divided into two sub-arrays, the first consisting of “odd” numbered detectors and the second consisting of “even” numbered detectors and are referred as the “odd” and “even” sub-arrays, respectively. The arrival direction of an EAS is then determined independently by the two sub-arrays. Since the detectors in the odd-even sub-array have a very substantial spatial overlap, they provide similar estimate of the EAS direction. The space angle between the “odd” and “even” directions ($\psi_{\text{odd/even}}$) involves the contribution of errors due to two independently reconstructed directions from two sub-arrays. Therefore, the error measured by the combination of the odd and even sub-arrays (σ_{oe}) is given by, $\sigma_{\text{oe}} = \sqrt{\sigma_o^2 + \sigma_e^2}$ where σ_o and σ_e are the angular resolutions for the odd and even sub-arrays, respectively. Since the odd and even sub-arrays are nearly identical and the number of detectors triggered in both cases typically are very similar, $\sigma_o = \sigma_e$ and therefore the angular resolution of the each sub-array would be equal to $\frac{\sigma_{\text{oe}}}{\sqrt{2}}$. Since the total number of detectors triggered in the full array would be double of the number in each sub-array, the angular resolution of the full array would be smaller by another factor of $\sqrt{2}$. By using this logic, the angular resolution of the array is estimated to be 1.2° for $N_e > 10^3$. After the iterative removal of the outliers the angular resolution improved to 0.8° for $N_e > 10^3$. It should be noted that this method is not sensitive to the shower front curvature as the two reconstructed directions are unaffected because both reconstructed directions suffer from identical systematic errors that are eliminated while estimating the space angle ψ . Therefore, the value estimated through the odd-even method represents the best achievable angular resolution.

A more realistic measure of the angular resolution can be obtained through the left-right method. In this method, the array is divided into two sub-arrays by a line joining the shower core with the array center, called “left” and “right” sub-arrays. As in the previous example, the arrival directions are determined independently by using these two sub-arrays and the angular resolution of each sub-array is $\frac{\sigma_{\text{lr}}}{2\sqrt{2}}$. Since the angular resolution is inversely proportional to the linear dimension of the array, we expect the angular resolution to worsen by an additional factor of $1/\sqrt{2}$ in the case of left-right method when compared to the odd-even method. Therefore, the additional

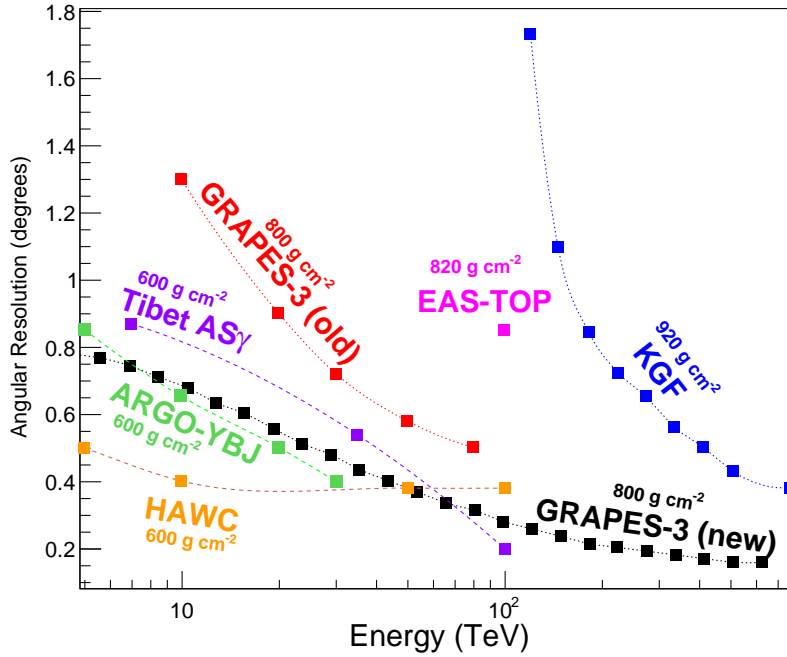


Figure 5: Variation of angular resolution with cosmic ray energy for various EAS experiments (adapted from [6]). Also shown are the atmospheric depths at which the experiments are located.

factor of $1/\sqrt{2}$ is used above. The angular resolution of the full array is given by, $\frac{\sigma_{tr}}{2\sqrt{2}}$. Since this method is sensitive to the systematic effects caused by curvature of the shower front, a planar fit to the arrival times yields an angular resolution 2° for $N_e > 10^3$ which is significantly larger than the angular resolution obtained by the odd-even method. The correction for the conical shower front led to a significant improvement in the angular resolution of the array, and the iterative elimination of outliers led to a final angular resolution of 0.8° for $N_e > 10^3$.

The angular resolution of the GRAPES-3 array was also calculated through Monte Carlo simulations. A total of 10^9 CORSIKA generated EAS were reconstructed to obtain their size, core location and arrival direction etc. The signal produced in the scintillator slab by the shower particles was then estimated with the aid of GEANT-4 based detector simulation. The timing response of the scintillator slab was simulated by using the observed distribution due to single muons. The angular resolution obtained by comparing the true arrival direction with the reconstructed arrival direction is 0.9° for $N_e > 10^3$. It is to be noted that this method of estimation of the angular resolution suffers from the limitations caused by the approximations inherent in a Monte Carlo simulation code such as CORSIKA and in the simulated response of the GRAPES-3 detectors.

The variation of angular resolution of GRAPES-3 array with the energy of the primary cosmic rays is shown in Fig. 5. The angular resolution is 0.8° at energies $E > 5$ TeV and improves to 0.3° at $E > 100$ TeV and finally approaching 0.16° at $E > 500$ TeV. Also shown in the same figure is the angular resolution of several other EAS experiments, as well as the angular resolution of the GRAPES-3 array obtained using the older technique. The older technique yielded an angular resolution of 1.3° at energies $E > 10$ TeV, which is significantly larger than the value obtained in the present work by a factor of ~ 1.6 . It is to be mentioned that the angular resolution of GRAPES-3

is comparable to that of the ARGO-YBJ and Tibet AS γ experiments, despite the fact that these two experiments are located at 200 g.cm⁻² shallower depth than Ooty.

5. Conclusion

In this work, the arrival times were initially corrected for the fixed times caused by the cables connecting the individual detectors to their respective HPTDCs. The arrival times were also corrected based on the distance from the shower core, depending on the slope of its shower front, which was observed to be varying with slope and age. The observations highlight the fact that for the same atmospheric depth, the present method of shower front curvature correction yields a significantly better angular resolution. It is expected that this improved angular resolution will result in an increased sensitivity towards the detection of new multi-TeV γ sources.

6. Acknowledgement

We acknowledge support of the Department of Atomic Energy, Government of India, under Project Identification No. RTI4002. This work was partially supported by grants from Chubu University, Japan. We are grateful to D.B. Arjunan, A.S. Bosco, V. Jeyakumar, S. Kingston, N.K. Lokre, K. Man- junath, S. Murugapandian, S. Pandurangan, B. Rajesh, R. Ravi, V. Santhoshkumar, S. Sathyaraj, M.S. Shareef, C. Shobana, and R. Sureshkumar for their role in efficient running of the experiment.

References

- [1] B.S. Acharya et al., *Angular resolution of the KGF experiment to detect ultra high energy gamma-ray sources*, J. Phys. G Nucl. Part. Phys. **19** (1993) 1053.
- [2] S. K. Gupta et al., *GRAPES-3–A high-density air shower array for studies on the structure in the cosmic-ray energy spectrum near the knee*, Nucl. Instrum. Meth. A **540** (2005) 311.
- [3] S.K. Gupta et al., *Measurement of arrival time of particles in extensive air showers using TDC32*, Expt. Astron. **35** (2012) 507.
- [4] H.H. He et al., *Detector time offset and off-line calibration in EAS experiments*, Astroparticle Physics **27** (2007) 528.
- [5] Souvik Das, *A simple alternative to the Crystal Ball function*, arxiv:1603.08591 (2016).
- [6] V.B. Jhansi et al, *The angular resolution of GRAPES-3 EAS array after improved timing and shower front curvature correction based on age and size*, Journal of Cosmology and Astroparticle Physics, **2020** (2020) 024.
- [7] V.B. Jhansi et al, *Precision measurement of arrival times in an EAS by GRAPES-3 experiment*, 35th International Cosmic Ray Conference (ICRC2017), **301** (2017) 354.